CRYSTAL GROWTH & DESIGN

pubs.acs.org/crystal

Communication

Terahertz Vibrational Motions Mediate Gas Uptake in Organic Clathrates

Wei Zhang, Zihui Song, Michael T. Ruggiero,* and Daniel M. Mittleman*

Cite This: *Cryst. Growth Des.* 2020, 20, 5638−5643

Read Online

ACCESS | Metrics & More | Article Recommendations | Supporting Information

ABSTRACT: Clathrates, supramolecular materials that contain guest molecules trapped within a framework of a host lattice, are important in many areas of science and technology. However, despite much research, fundamental questions concerning the mechanism and kinetics associated with the enclathration process remain unanswered. Here, through a combination of terahertz spectroscopy, density functional theory, and molecular dynamics simulations, we demonstrate that the gas-capture process is mediated by a single terahertz vibrational mode and then use this mode to track the uptake of gas. This result provides a critical molecular-level understanding of this key kinetic process in clathrate science.

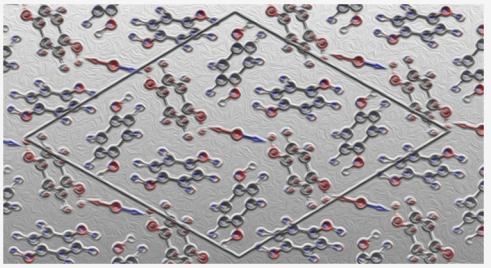

The study of clathrates has a long history, owing to their widespread abundance and their exceptional physical and chemical properties.[1−4] One of the most widely studied clathrates is methane hydrate clathrate, also known as natural gas hydrate (NGH), a naturally occurring material in which methane is caged within a water framework.[5] It has been estimated that the amount of methane stored in naturally occurring NGH is sufficient to support global energy needs for many years.[6] In addition, clathrates are finding use in a wide number of applications, including areas related to hydrogen storage,[4,7] separations,[3] photovoltaics,[1] and thermoelectrics.[2] While the applications of clathrate systems are steadily increasing, the widespread exploitation of such materials relies on a thorough understanding of the atomic-level processes that dictate and drive gas capture and selective uptake. A key example is the gas-adsorption reaction, which has been studied extensively from both an experimental and theoretical perspective.[7−9] However, the mechanism and kinetics of clathrate reactions represent one of the most important and least thoroughly addressed aspects of the physics of clathrates.

Hydroquinone (HQ) is known to form a prototypical organic clathrate that has been the subject of extensive study. HQ is a phenolic compound of formula p-$C_6H_4(OH)_2$, with the clathrate formation driven by the assembly of hydrogen-bonded rings. It has at least four polymorphs;[10] two of these, the α- and β-forms, are most commonly observed, and both form clathrate structures. The α-polymorph[11] is the most stable structure under ambient conditions and forms crystals with a hexagonal unit cell ($R\bar{3}$ space group) containing 54 HQ molecules, with one pore for every 18 HQ molecules (Figure 1a), representing a porosity of 2.84%. On the other hand, the β-form, which also crystallizes in the $R\bar{3}$ space group,[12] represents a more accessible clathrate structure, with one pore for every three HQ molecules and a porosity of 15.07%. The pores are formed by hydrogen bonded rings, with the accessible spherical-like cages having diameters of about 4 Å,[13] which may (or may not) be occupied by small guest molecules to form clathrates (Figure 1b). The guest-free-β-HQ form is highly selective in the guest-capturing kinetics, making it a promising candidate for selective gas separation and storage.[14,15] HQ frameworks have also been recognized as being valuable for hydrogen storage[4,16] as well as serving as a platform for studying the dynamics of confined guest molecules.[17,18] Numerous theoretical and experimental studies have been performed to understand the properties of α- and β-HQ, including the dynamics and kinetics involved in the capture, release, and diffusion of guest molecules, some dating back over 50 years.[19] Methods including X-ray diffraction, Raman spectroscopy, nuclear magnetic resonance spectroscopy, and terahertz spectroscopy have been used for measuring the formation and decomposition rates of various types of HQ clathrates.[8,14,20] However, these studies provided little atomic-level insight regarding the specific dynamics involved. There have also been computational studies based on molecular dynamics simulations,[4,7] but these primarily focused on the energetics involved with enclathration and the structure of the HQ cavities upon adsorption, rather than on the dynamics of the guest molecules and their capture.

Low-frequency (terahertz) vibrations (0.1−10 THz, 3−333 cm^{-1}) have long been understood to be related to many phenomena in solid-state materials, driving properties such as thermal expansion, elasticity, and stability, to name a few.[21−23]

Received: June 10, 2020
Revised: July 23, 2020
Published: July 23, 2020

https://dx.doi.org/10.1021/acs.cgd.0c00797
Cryst. Growth Des. 2020, 20, 5638−5643

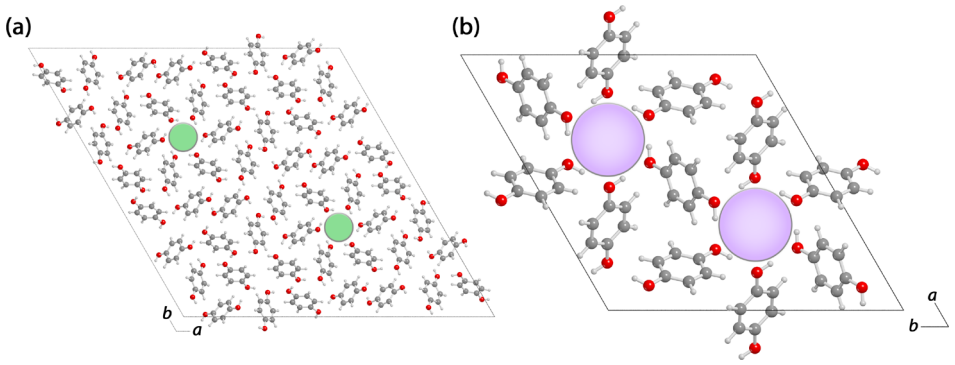

Figure 1. Crystal structure of (a) α-HQ and (b) β-HQ, with the pores highlighted.

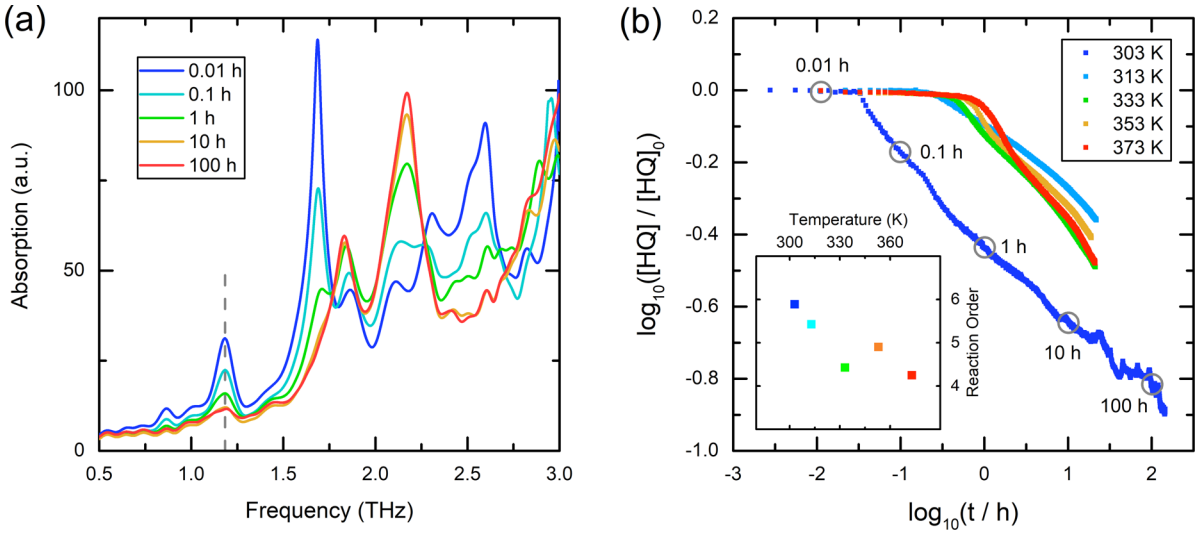

Figure 2. Experimental characterization of the transition from α-HQ to β-HQ-CO_2. (a) THz spectra at various time intervals over the course of the reaction. The vertical dashed line corresponds to the peak used to track the reaction. (b) Temperature-dependent kinetics of the transition from α-HQ to β-HQ-CO_2. The horizontal axis shows the time elapsed from the initial contact of HQ and pressurized CO_2. The vertical axis shows the relative amount of HQ. Inset: Reaction order of the second stage for different temperatures.

As a result, terahertz spectroscopy has proven to be a powerful technique for the study of solids, as the modes in this low-frequency range are incredibly sensitive to the bulk structure and to the weak forces, which can ultimately determine the thermodynamics and phase behavior. Recently, an explicit connection between specific terahertz vibrations and phase-transformation phenomena has been uncovered in organic solids, enabling the elucidation of the mechanism and kinetics of this process with unprecedented clarity.[24] Using terahertz time-domain spectroscopy (THz-TDS), spectra can be acquired across a wide range of tuning parameters, including our recently developed approach to pressure-dependent spectroscopy up to 35 MPa.[25] We have recently applied this combined methodology to study metal−organic frameworks (MOFs), another class of porous materials that are similar to clathrates in both structure and function. In the prototypical MOF compound, ZIF-8, the guest-capture and guest-release processes are related to low-frequency phonon modes of the framework, which can be observed with THz-TDS.[23]

In light of these new advances, coupled with previous studies that have utilized terahertz techniques to study clathrates,[26−29] this study focuses on utilizing pressure-dependent THz-TDS to understand the low-frequency dynamics related to gas capture in hydroquinone (HQ) clathrates. α-HQ (≥99.5%, obtained from Sigma-Aldrich and used without further purification) is compressed into tablets with diameters of 6 mm and thicknesses of approximately 0.2 mm. The HQ tablets are attached to thick polyethylene spacers with diameters of 6 mm and thicknesses of around 2.3 mm to increase the path length of the THz radiation and suppress the effects of etalon reflections in the sample. These tablets are then placed into a custom-designed pressure cell, with a window for THz access.[25] The preactivated samples are prepared with an extra step of vacuuming with a pressure of below 5 Pa at room temperature for 24 h prior to the CO_2 reaction. For the reaction, compressed CO_2 (≥99.99, 850 psi (58.6 bar), TechAir) is conducted into the pressure cell. β-HQ-CO_2 was generated by CO_2 pressurization, with total conversion achieved after several days. A liquid nitrogen coldfinger and an electric heater are used to accurately control the sample temperature, with an accuracy of around 0.1 K, which has been calibrated using the phase transitions of known materials (nitrogen, argon, and methane) under different pressures.

We use a commercial THz time-domain spectrometer (Toptica Teraflash Pro) to measure THz spectra inside the pressure cell and monitor the spectral changes of the sample throughout the reaction. In the data analysis, we use an asymmetric tapered cosine window with a length of

https://dx.doi.org/10.1021/acs.cgd.0c00797
Cryst. Growth Des. 2020, 20, 5638−5643

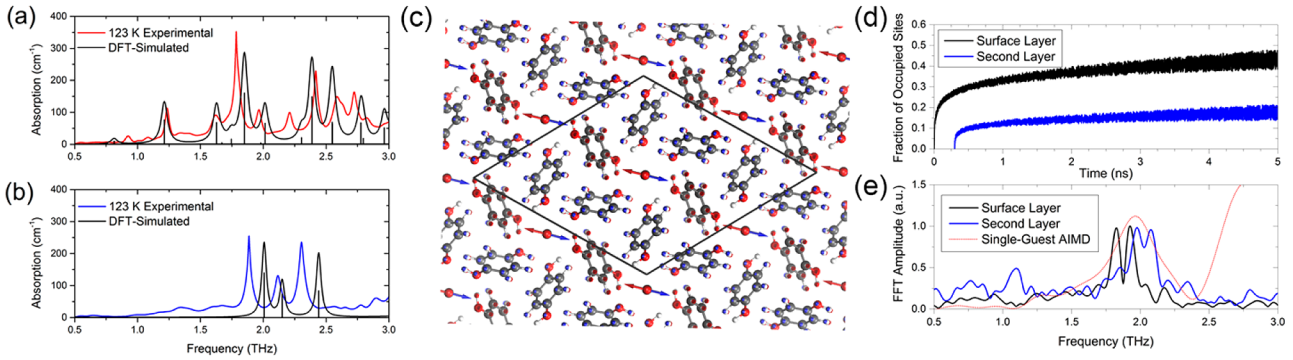

Figure 3. Atomic-level dynamics of the studied materials. Measured low-temperature THz-TDS spectra for (a) α-HQ (red) and (b) β-HQ-CO_2 (blue), together with the predicted (black) spectra, from DFT calculations, and (c) the eigenvector displacements (positive and negative directions as blue and red, respectively) for the 2.01 THz mode in β-HQ-CO_2 predicted using solid-state DFT simulations. (d) The MD-predicted adsorption curves for the first (surface; black) and second (blue) layers of cavities in β-HQ and (e) the FFT of those absorption curves, showing significant spectral intensity near the predicted "cage-rattling" mode of the CO_2 molecules within the solid. Also shown is a dotted-red curve corresponding to the AIMD-predicted vibrational dynamics of a single CO_2 molecule within an otherwise empty HQ-host lattice, again showing a broad feature around 2 THz.

approximately 16 ps to truncate the time-domain waveform to remove the multiple reflections in the cell's diamond window, and then zero-pad to a total of 131 072 points, and Fourier transform the waveforms to obtain the THz spectra of the sample. The spectrum of a pure polyethylene tablet is also measured, as the reference against which other spectra are normalized.

Given the distinct differences between the respective structures of the two crystals and the corresponding differences to the THz-TDS spectra,[30] it is possible to track the transition from one solid to the other as pressure is applied to the sample using THz-TDS alone (Figure 2). By monitoring the THz spectral change, we can track the kinetics of the reaction from α-HQ to β-HQ-CO_2. In particular, the relative amount of HQ is obtained by tracking the absorption coefficient of the sample at 1.18 THz, corresponding to the first phonon mode of α-HQ. Since this peak does not appear in the β-form, it is a useful marker for the conversion of the sample to the clathrate. We observe that this reaction occurs in two distinct stages (Figure 2b). The first is the activation stage, where the reaction proceeds slowly even though the reactants (HQ and CO_2) are in contact and the reaction is thermodynamically favored. The duration of this first stage mainly depends on the preprocessing (or preactivation) of the HQ sample, which removes the guest molecules (e.g., CO_2, N_2, noble gases, and so on) that occupy the surface layer. For MOF compounds, this preactivation step has been identified to be important for the removal of guest molecules without compromising the pore structure.[31] If the sample is not preactivated, then the duration of the activation stage in our experiment is between 20 and 40 min, depending on the reaction temperature (with higher temperature corresponding to a longer duration). However, if the sample is stored under vacuum for 24 h prior to pressurization with CO_2, then the duration of the activation stage drastically reduces to below 2 min. In the second stage, the reaction rate suddenly increases.

As noted, it is sensible to separate this kinetic process into two distinct stages. We define the transition point as the time when 5% of the α-HQ is consumed. The reaction orders in the second stage are extracted by fitting the second stage data to an order-based kinetic model $d\alpha/dt = -k\alpha n$, where α is the relative amount of HQ (normalized by the initial amount), t is time, k is the reaction rate constant, and n is the reaction order.[32] We obtain a reaction order of around 5 (Figure 2b, inset).

In order to study the role of low-frequency dynamics on these adsorption processes, the atomic-level dynamics are explored using computational means. The experimental THz-TDS spectra of the two studied crystals are shown in Figure 3, along with the previously published DFT-predicted spectra.[30] The vibrational motions occurring at terahertz frequencies in α-HQ represent predominantly external librations of the HQ molecules, with the large number of symmetry-independent atoms yielding numerous degrees of freedom and thus a complex set of vibrational motions involving many molecules simultaneously. In the case of β-HQ-CO_2, the mode structure is much less complex; the first two peaks correspond to hindered translations and rotations of the CO_2 molecules alone within the pore, while the third feature at the highest frequency corresponds to a coupled motion between the CO_2 guest molecule and the HQ host. Of particular interest is the highest-frequency mode in β-HQ-CO_2 (Figure 3c), as this represents the motion of only the enclathrated gas molecules.

The assignment of the terahertz spectra and identification of the particular dynamics do not provide much information related to the adsorption process on their own. Thus, we perform molecular dynamics (MD) simulations to explore the atomic dynamics during adsorption of CO_2 by HQ. However, the complete conversion process, from the unoccupied α-HQ crystal to the fully occupied β-HQ-CO_2, represents a major challenge to computational modeling, as it involves complicated and nonuniform intermediate structures and reorganization of the bulk structure. Therefore, we have chosen to study the final step(s), namely, gas uptake by an empty β-HQ-CO_2 lattice. Simulations were performed using GROMACS[33] with the OPLS-AA force field[34] according to standard methodologies[7] in the NPT ensemble at 300 K, and a time step of 1 fs was used. Given previous success, an anisotropic pressure coupling was used, with a doubled coupling constant value along the gas−crystal interface. The cutoffs for the Coulomb and Lennard-Jones potentials were set to 2 nm. The loading curves were generated by determining the occupation of the guest sites by gas molecules, when the gas was within a sphere with a diameter of 4.0 Å within the host cage. We model a finite 5.74 nm-thick β-HQ slab, with side lengths of 6.63 nm by 6.63 nm in a 6.63 nm × 6.63 nm × 10.00 nm simulation cell.

https://dx.doi.org/10.1021/acs.cgd.0c00797
Cryst. Growth Des. 2020, 20, 5638−5643

After an initial equilibration period, excess CO_2 molecules are introduced into the void space above and below the HQ slab, and production trajectories are obtained.

The results, shown in Figure 3d, demonstrate that CO_2 molecules begin to adsorb into the first layer of pores in the HQ solid very rapidly, in line with similar simulations[7] on hydrogen capture by β-HQ-H_2. Around 300 ps, the enclathrated guests begin to diffuse deeper into the solid but at a much slower rate (blue curve in Figure 3d). It is important to note that the effective pressure of the gas molecules is higher in the simulation than what we achieve in the corresponding experiment (ca. 221 and 59 bar, respectively), and the simulated material is significantly thinner than the experimental sample (which consists of micro- to nanocrystalline particles), yielding a large surface-to-bulk ratio. Nevertheless, these simulations provide important insights into the interaction of the gas molecules with the clathrate material. One clear observation is that the loading of the first few surface layers occurs relatively quickly, while penetration deeper into the crystal is significantly slower, likely due to steric hindrance. This helps to explain the experimental observation of two distinct adsorption stages. It also suggests an explanation for the distinct behavior of the preactivated samples; in those materials, the surface cavities are likely emptied by the storage under vacuum as well as the formation of a metastable (and likely disordered) surface structure, as observed in the dehydration of pharmaceutical hydrates,[35] which leads to an initial rapid uptake of guests. As the processes proceed and gas penetrates into the interior of the crystal, the reaction proceeds more slowly, with a second, much smaller, rate constant.

A close inspection of the generated MD trajectories shows an additional feature, which is extremely interesting. Throughout the simulation, CO_2 molecules move in and out of the first layer of clathrate sites, leading to apparent "noise" in the simulated adsorption curve (Figure 3d). In order to determine if this process is random or related to a deterministic phenomenon, we perform a Fourier transform of the adsorption curves for the surface and second layers. The result is shown in Figure 3e. We observe two closely spaced peaks in this spectrum, located at a frequency close to 2 THz, with the internal adsorption curve yielding a slightly blue-shifted peak compared to the surface sites. Interestingly, these peaks are at nearly the same frequencies as modes identified in both the experimental and static-DFT simulated vibrational spectra. In particular, they appear to be coincident with the "cage-rattling" modes of the enclathrated CO_2 molecule within the cavity; this mode, predicted to lie at 2.01 THz, is illustrated in Figure 3c. Analysis of the adsorption dynamics suggests that, once the CO_2 molecules become enclathrated, they begin to experience a vibrational potential corresponding to what is observed in bulk HQ-CO_2. Due to the close proximity of the enclathrated CO_2 and the gaseous CO_2, some coupling between the two can occur, likely due to weak dipole-coupling and other van der Waals interactions. As the enclathrated CO_2 experiences more long-range motion (i.e., beyond local oscillations around its potential energy minima) and diffuses further into the solid, similar in nature to metabasin transitions in amorphous solids,[36,37] the coupling between the two CO_2 species (free and enclathrated) aids in the adsorption process of additional molecules through a favorable interaction with the transient void created by the diffusing enclathrated CO_2 molecule. This could lead to a shuttling effect, which is similar to what has been observed in the case of proton transfer in biomolecular systems.[38] Thus, one would expect a strong correlation between the oscillatory motion of the initial enclathrated CO_2 molecules with the unincorporated molecules. Our results provide clear evidence that a particular terahertz motion is implicated in this enclathration process.

In the terahertz range, narrow and well-resolved vibrational features in solids are typically pictured as arising from delocalized motions that occur throughout the periodic solid with long-range order (i.e., phonons).[39] It may therefore seem somewhat surprising that a single molecule appears to undergo vibrational motion at the same, or nearly the same, frequency as bulk HQ-CO_2. In order to further investigate this, we perform ab initio molecular dynamics (AIMD) simulations using CP2k[40] on a β-HQ supercell ($3 \times 3 \times 3$) with only one CO_2 site occupied in the central unit cell and three-dimensional periodic boundary conditions applied. The PBE-D3 functional was again used, with a triple-ζ basis set,[41] in order to be similar to the static-DFT simulations.[30] The simulations were performed with a time step of 0.5 fs in the NVT ensemble, with the temperature set to 300 K. The generated IR spectrum was obtained by taking the Fourier transform of the dipole moment autocorrelation function, where the dipoles were calculated using the localized Wannier function approach.[23,42] The results (Figure 3e, red curve) show that a single enclathrated CO_2 molecule does indeed exhibit transitions that mirror those observed in the bulk extended crystal. The origins of this result are likely rooted in the very weak potential energy landscape in which the trapped CO_2 molecules exist. The only significant intermolecular interaction between the host and guest are weak van der Waals forces, with little coupling between adjacent porous sites. This result supports our description of the enclathration kinetics, as a single molecule clearly undergoes oscillatory motion at the same (or nearly the same) frequency as a fully enclathrated species.

Using a combination of experimental temperature- and pressure-dependent THz-TDS, quantum mechanical calculations, and classical simulations, we provide a consistent description of the transition between empty HQ and HQ clathrate in the presence of high-pressure CO_2 gas. We are able to identify a specific vibrational mode that is directly linked to the gas uptake kinetics. This represents the first case in clathrate science in which a reaction coordinate has been identified for the guest capture reaction and directly mapped to a particular low-frequency vibrational mode and opens the door for future studies into the exciting possibility of using terahertz radiation to promote phase-change processes in porous materials, as previously shown for other organic solids.[43,44]

■ ASSOCIATED CONTENT

Supporting Information

The Supporting Information is available free of charge at https://pubs.acs.org/doi/10.1021/acs.cgd.0c00797.

Density functional theory input files (ZIP)

■ AUTHOR INFORMATION

Corresponding Authors

Michael T. Ruggiero − *Department of Chemistry, University of Vermont, Burlington, Vermont 05405, United States;* orcid.org/0000-0003-1848-2565; Email: michael.ruggiero@uvm.edu

https://dx.doi.org/10.1021/acs.cgd.0c00797
Cryst. Growth Des. 2020, 20, 5638−5643

Daniel M. Mittleman − *School of Engineering, Brown University, Providence, Rhode Island 02912, United States;* orcid.org/0000-0003-4277-7419; Email: daniel_mittleman@brown.edu

Authors

Wei Zhang − *School of Engineering, Brown University, Providence, Rhode Island 02912, United States*

Zihui Song − *Department of Chemistry, University of Vermont, Burlington, Vermont 05405, United States*

Complete contact information is available at: https://pubs.acs.org/10.1021/acs.cgd.0c00797

Notes

The authors declare no competing financial interest.

REFERENCES

(1) Martinez, A. D.; Krishna, L.; Baranowski, L. L.; Lusk, M. T.; Toberer, E. S.; Tamboli, A. C. Synthesis of Group IV clathrates for photovoltaics. *IEEE J. Photovolt.* **2013**, *3*, 1305−1310.

(2) Takabatake, T.; Suekuni, K.; Nakayama, T.; et al. Phonon-glass electron-crystal thermoelectric clathrates: Experiments and theory. *Rev. Mod. Phys.* **2014**, *86*, 669−716.

(3) Fink, J. *Petroleum engineer's guide to oil field chemicals and fluids*; 2nd ed.; Elsevier: 2015.

(4) Daschbach, J. L.; Chang, T. M.; Corrales, L. R.; Dang, L. X.; McGrail, P. Molecular mechanisms of hydrogen-loaded beta-hydroquinone clathrate. *J. Phys. Chem. B* **2006**, *110*, 17291−17295.

(5) Sloan, E. D. Fundamental principles and applications of natural gas hydrates. *Nature* **2003**, *426*, 353.

(6) Li, X. S.; Xu, C. G.; Zhang, Y.; Ruan, X. K.; Li, G.; Wang, Y. Investigation into gas production from natural gas hydrate: A review. *Appl. Energy* **2016**, *172*, 286−322.

(7) Perez-Rodriguez, M.; Otero-Fernandez, J.; Comesana, A.; Fernandez-Fernandez, A. M.; Pineiro, M. M. Simulation of capture and release processes of hydrogen by beta-hydroquinone clathrate. *ACS Omega* **2018**, *3*, 18771−18782.

(8) Coupan, R.; Pere, E.; Dicharry, C.; Torré, J. P. New insights on gas hydroquinone clathrates using *in situ* Raman spectroscopy: Formation/dissociation mechanisms, kinetics, and capture selectivity. *J. Phys. Chem. A* **2017**, *121*, 5450−5458.

(9) Lee, J.; Kim, K.-S.; Seo, Y. Thermodynamic, structural, and kinetic studies of cyclopentane+CO_2 hydrates: Applications for desalination and CO_2 capture. *Chem. Eng. J.* **2019**, *375*, 121974.

(10) Naoki, M.; Yoshizawa, T.; Fukushima, N.; Ogiso, M.; Yoshino, M. A new phase of hydroquinone and its thermodynamic properties. *J. Phys. Chem. B* **1999**, *103*, 6309−6313.

(11) Wallwork, S. C.; Powell, H. M. The crystal structure of the a form of quinol. *J. Chem. Soc., Perkin Trans. 2* **1980**, *2*, 641−646.

(12) Torré, J. P.; Coupan, R.; Chabod, M.; Pere, E.; Labat, S.; Khoukh, A.; Brown, R.; Sotiropoulos, J. M.; Gornitzka, H. CO_2-hydroquinone clathrate: Synthesis, purification, characterization and crystal structure. *Cryst. Growth Des.* **2016**, *16*, 5330−5338.

(13) Hermansson, K. Host-guest interactions in an organic crystal: beta-hydroquinone clathrate with Ne and HF guests. *J. Chem. Phys.* **2000**, *112*, 835−840.

(14) Lee, Y. J.; Han, K. W.; Jang, J. S.; Jeon, T. I.; Park, J.; Kawamura, T.; Yamamoto, Y.; Sugahara, T.; Vogt, T.; Lee, J. W.; Lee, Y.; Yoon, J. H. Selective CO_2 trapping in guest-free hydroquinone clathrate prepared by gas-phase synthesis. *ChemPhysChem* **2011**, *12*, 1056−1059.

(15) Coupan, R.; Dicharry, C.; Torré, J. P. Hydroquinone clathrate based gas separation (HCBGS): Application to the CO_2/CH_4 gas mixture. *Fuel* **2018**, *226*, 137−147.

(16) van den Berg, A. W.; Arean, C. O. Materials for hydrogen storage: current research trends and perspectives. *Chem. Commun.* **2008**, *14*, 668−681.

(17) Takeda, S.; Kataoka, H.; Shibata, K.; Ikeda, S.; Matsuo, T.; Carlile, C. J. Quantum precession of HCl molecule in hydroquinone clathrate. *Phys. B* **1994**, *202*, 315−319.

(18) Strobel, T. A.; Ramirez-Cuesta, A. J.; Daemen, L. L.; Bhadram, V. S.; Jenkins, T. A.; Brown, C. M.; Cheng, Y. Q. Quantum dynamics of H_2 trapped within organic clathrate cages. *Phys. Rev. Lett.* **2018**, *120*, 120402.

(19) Mandelcorn, L. *Chem. Rev.* **1959**, *59*, 827−839.

(20) Lee, J. W.; Choi, K. J.; Lee, Y.; Yoon, J. H. Spectroscopic identification and conversion rate of gaseous guest-loaded hydroquinone clathrates. *Chem. Phys. Lett.* **2012**, *528*, 34−38.

(21) Sibik, J.; Löbmann, K.; Rades, T.; Zeitler, J. A. Predicting crystallization of amorphous drugs with terahertz spectroscopy. *Mol. Pharmaceutics* **2015**, *12*, 3062−3068.

(22) Ruggiero, M. T.; Zeitler, J. A.; Erba, A. Intermolecular anharmonicity in molecular crystals: interplay between experimental low-frequency dynamics and quantum quasi-harmonic simulations of solid purine. *Chem. Commun.* **2017**, *53*, 3781−3784.

(23) Zhang, W.; Maul, J.; Vulpe, D.; Moghadam, P. Z.; Fairen-Jimenez, D.; Mittleman, D. M.; Zeitler, J. A.; Erba, A.; Ruggiero, M. T. Probing the mechanochemistry of metal-organic frameworks with low-frequency vibrational spectroscopy. *J. Phys. Chem. C* **2018**, *122*, 27442−27450.

(24) Ruggiero, M. T.; Zhang, W.; Bond, A. D.; Mittleman, D. M.; Zeitler, J. A. Uncovering the connection between low-frequency dynamics and phase transformation phenomena in molecular solids. *Phys. Rev. Lett.* **2018**, *120*, 196002.

(25) Zhang, W.; Nickel, D.; Mittleman, D. High-pressure cell for terahertz time-domain spectroscopy. *Opt. Express* **2017**, *25*, 2983−2993.

(26) Burgiel, J. C.; Meyer, H.; Richards, P. L. Far-infrared spectra of gas molecules trapped in β-quinol clathrates. *J. Chem. Phys.* **1965**, *43*, 4291−4299.

(27) Takeya, K.; Zhang, C. H.; Kawayama, I.; Murakami, H.; Jepsen, P. U.; Chen, J.; Wu, P. H.; Ohgaki, K.; Tonouchi, M. Terahertz time domain spectroscopy for structure-II gas hydrates. *Appl. Phys. Express* **2009**, *2*, 122303.

(28) Jang, J. S.; Jeon, T.-I.; Lee, Y. J.; Yoon, J. H.; Lee, Y. Characterization of alpha-hydroquinone and beta-hydroquinone clathrates by THz time-domain spectroscopy. *Chem. Phys. Lett.* **2009**, *468*, 37−41.

(29) Lee, E. S.; Han, K. W.; Yoon, J. H.; Jeon, T.-I. Probing structural transition and guest dynamics of hydroquinone clathrates by temperature-dependent terahertz time-domain spectroscopy. *J. Phys. Chem. A* **2011**, *115*, 35−38.

(30) Zhang, W.; Song, Z.; Ruggiero, M. T.; Mittleman, D. M. Assignment of terahertz modes in hydroquinone clathrates. *J. Infrared, Millimeter, Terahertz Waves* **2020**, in press; DOI: 10.1007/s10762-020-00670-w

(31) Mondloch, J. E.; Karagiaridi, O.; Farha, O. K.; Hupp, J. T. Activation of metal-organic framework materials. *CrystEngComm* **2013**, *15*, 9258−9264.

(32) Khawam, A.; Flanagan, D. R. Solid-state kinetic models: Basics and mathematical fundamentals. *J. Phys. Chem. B* **2006**, *110*, 17315−17328.

(33) Pronk, S.; Páll, S.; Schulz, R.; Larsson, P.; Bjelkmar, P.; Apostolov, R.; Shirts, M. R.; Smith, J. C.; Kasson, P. M.; Spoel, D. v. d.; Hess, B.; Lindahl, E. GROMACS 4.5: a high-throughput and highly parallel open source molecular simulation toolkit. *Bioinformatics* **2013**, *29*, 845−854.

(34) Jorgensen, W. L.; Maxwell, D. S.; Tirado-Rives, J. Development and testing of the OPLS all-atom force field on conformational energetics and properties of organic liquids. *J. Am. Chem. Soc.* **1996**, *118*, 11225−11236.

(35) Larsen, A. S.; Ruggiero, M. T.; Johansson, K. E.; Zeitler, J. A.; Rantanen, J. Tracking dehydration mechanisms in crystalline hydrates with molecular dynamics simulations. *Cryst. Growth Des.* **2017**, *17*, 5017−5022.

(36) Cicerone, M. T.; Tyagi, M. Metabasin transitions are Johari-Goldstein relaxation events. *J. Chem. Phys.* **2017**, *146*, No. 054502.
(37) Cao, P.; Short, M. P.; Yip, S. Potential energy landscape activations governing plastic flows in glass rheology. *Proc. Natl. Acad. Sci. U. S. A.* **2019**, *116*, 18790−18797.
(38) Agback, P.; Agback, T. Direct evidence of a low barrier hydrogen bond in the catalytic triad of a Serine protease. *Sci. Rep.* **2018**, *8*, 10078.
(39) Nickel, D. V.; Ruggiero, M. T.; Korter, T. M.; Mittleman, D. M. Terahertz disorder-localized rotational modes and lattice vibrational modes in the orientationally-disordered and ordered phases of camphor. *Phys. Chem. Chem. Phys.* **2015**, *17*, 6734−6740.
(40) Hutter, J.; Iannuzzi, M.; Schiffmann, F.; Vandevondele, J. cp2k: Atomistic simulations of condensed matter systems. *WIREs Comput. Mol. Sci.* **2014**, *4*, 15−25.
(41) VandeVondele, J.; Hutter, J. Gaussian basis sets for accurate calculations on molecular systems in gas and condensed phases. *J. Chem. Phys.* **2007**, *127*, 114105.
(42) Thomas, M.; Brehm, M.; Fligg, R.; Vöhringer, P.; Kirchner, B. Computing vibrational spectra from *ab initio* molecular dynamics. *Phys. Chem. Chem. Phys.* **2013**, *15*, 6608−6622.
(43) Ruggiero, M. T.; Krynski, M.; Kissi, E. O.; Sibik, J.; Markl, D.; Tan, N. Y.; Arslanov, D.; van der Zande, W.; Redlich, B.; Korter, T. M.; Grohganz, H.; Lobmann, K.; Rades, T.; Elliott, S. R.; Zeitler, J. A. The significance of the amorphous potential energy landscape for dictating glassy dynamics and driving solid-state crystallisation. *Phys. Chem. Chem. Phys.* **2017**, *19*, 30039−30047.
(44) Hoshina, H.; Suzuki, H.; Otani, C.; Nagai, M.; Kawase, K.; Irizawa, A.; Isoyama, G. Polymer Morphological Change Induced by Terahertz Irradiation. *Sci. Rep.* **2016**, *6*, 27180.

https://dx.doi.org/10.1021/acs.cgd.0c00797
Cryst. Growth Des. 2020, 20, 5638−5643